A reproduction of boundary conditions in three-dimensional continuous casting problem

Iwona Nowak, Jacek Smolka, and Andrzej J. Nowak

Abstract—The paper discusses a 3D numerical solution of the inverse boundary problem for a continuous casting process of alloy. The main goal of the analysis presented within the paper was to estimate heat fluxes along the external surface of the ingot. The verified information on these fluxes was crucial for a good design of a mould, effective cooling system and generally the whole caster. In the study an enthalpy-porosity technique implemented in Fluent package was used for modeling the solidification process. In this method, the phase change interface was determined on the basis of the liquid fraction approach. In inverse procedure the sensitivity analysis was applied for retrieving boundary conditions. A comparison of the measured and retrieved values showed a high accuracy of the computations. Additionally, the influence of the accuracy of measurements on the estimated heat fluxes was also investigated.

Keywords—boundary inverse problem, sensitivity analysis, continuous casting, numerical simulation.

I. INTRODUCTION

THe continuous casting of metals, alloys, semiconductor crystals, etc., is nowadays a frequently utilized technology in a contemporary industry. Taking into account quality of the casting material, a possibility of the design as well as a control of the casting process is very important. For this reason, numerical models may be successfully used to analyze some phenomena and processes in continuous casting with relatively low costs. The quality of the casting material is dependent on a procedure of cooling and a speed of the casting process. Therefore, a decision was made to reconstruct the cooling conditions in the continuous casting on the basis of measurements at some points inside the ingot. This kind of problems is formulated as the inverse boundary problem and in the presented work is solved employing a sensitivity analysis. In the paper the heat flux distribution along the external boundary of an ingot was estimated. Similar problems were the subjects of works dealing with both the boundary and the geometry inverse problems to estimate the geometry of a body [1], [2], [3], [11]. However, the majority of them were formulated as two-dimensional problems, while in this project the three-dimensional continuous casting problem is discussed.

In this paper the heat flux distribution along the external boundary of 3-D model of ingot was estimated. In addition, the continuous casting of the aluminium alloy was considered. This resulted in modelling of mushy zones within computational domain. Moreover, a mathematical model included

Iwona Nowak Institute of Mathematics, Silesian University of Technology, Gliwice, Poland, email: iwona.nowak@polsl.pl

Jacek Smolka, Institute of Thermal Technology, Silesian University of Technology, Gliwice, Poland, email: jacek.smolka@polsl.pl

Andrzej J. Nowak, Institute of Thermal Technology, Silesian University of Technology, Gliwice, Poland, email: andrzej.nowak@polsl.pl

the momentum and the continuity equations apart from the energy equation. Such approach allowed one to analyze a natural convection in the liquid phase. In the mathematical description a thermal resistance along crystallizer was also taken into account. The thermal resistance between the ingot and crystallizer wall originates from a material contraction and is usually modelled as a constant value [10]. In this paper the thermal resistance is modelled as spatially local value determined on the basis of local temperatures of the ingot and crystallizer walls.

The computational procedure of retrieving the unknown values was carried out iteratively and required the following main steps in each loop:

- a solution of the direct problem using a commercial Finite Volume Method code Fluent [4]. In the first iteration the unknown parameters were assumed and the temperature field inside the body was determined. The study showed that an effectiveness of the procedure developed was independent on the initials values in a direct problem. Moreover, a number of the parameters as the under-relaxation factor, number of iterations in each cycle, value of the time step were investigated to significantly decrease the computational time of the direct case.

- a solution of the inverse problem using an in-house code for the sensitivity analysis. Once the adequate objective function was minimized, the obtained values of heat fluxes were implemented into Fluent by User Defined Function (UDF) [4]. The mathematical model of the performed computations had to be supplemented with appropriate temperature measurements. The thermal inverse analysis discussed in the paper was based on the temperature measurements collected by thermocouples immersed in the liquid metal, carried by the cast and finally pulled out by the solidified ingot [1], [5].

II. PROBLEM FORMULATION AND DIRECT PROBLEM

The geometrical model of the computational domain considered in the direct problem was in the shape of a brick with the following dimensions: 1.86 m x 0.51 m x 5.00 m, see Figure 1. Due to the symmetry of the object only one-fourth of it was analyzed. An influence of the numerical mesh generated within the geometry on the phase-change problem was investigated. Finally, the grid with almost 400 000 of hexahedral elements of very high quality was used in the inverse procedure.

The enthalpy-porosity technique was used in Fluent for modeling the phase change process [4], [6]. For this reason, the liquid fraction was computed at each iteration utilizing the
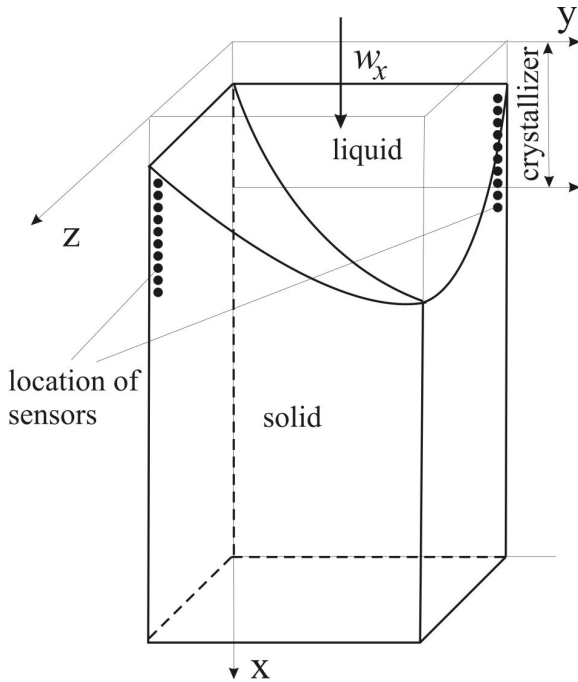
Fig. 1. Scheme of the 3D domain of the continuous casting system.

enthalpy balance. For the solidification problem studied, the energy equation could be expressed as:

$$\nabla \cdot (k\nabla T) = \boldsymbol{\nabla} \cdot \rho \boldsymbol{w} H + \frac{\partial}{\partial t}(\rho H) \qquad (1)$$

where k denotes the thermal conductivity, T stands for the temperature, ρ represents the density, w is the velocity vector, H denotes the enthalpy, and t is the time.

In the energy equation (1), the enthalpy of the material H was calculated as a sum of the sensible enthalpy and the latent heat:

$$H = h + \Delta H \qquad (2)$$

where h is the sensible enthalpy, and ΔH represents the latent heat. The sensible enthalpy h can be determined on the basis of the following equation:

$$h = h_{ref} + \int_{T_{ref}}^{T} c_p dT \qquad (3)$$

where h_{ref} denotes the reference enthalpy, T_{ref} is the reference temperature, and c_p stands for the specific heat at constant pressure.

The equation for the latent heat content ΔH can be written in terms of the latent heat of the material L:

$$\Delta H = \beta L \qquad (4)$$

where β is the liquid fraction and takes the following values:

$$\beta = 0 \qquad\qquad\quad \text{if} \quad T < T_S$$
$$\beta = (T - T_S)/(T_L - T_S) \quad \text{if} \quad T_S < T < T_L \qquad (5)$$
$$\beta = 1 \qquad\qquad\quad \text{if} \quad T > T_L$$

Apart from the energy equation (1), the mathematical model in the liquid phase included the momentum and the continuity equations to simulate the convective motions. Since the casting material was an alloy, the momentum equation was supplemented with additional source term describing a mushy zone region as a porous medium. To solve the set of equations governing the casing process of alloys, appropriate material properties for the aluminium alloy and boundary conditions were defined. The thermophysical properties of the considered aluminium alloy are strongly dependent on temperature. Therefore, the density, the dynamic viscosity and the thermal conductivity were defined using polynomial functions of temperature for a liquid phase, mushy zone and solid phase. Since the temperature dependence of the specific heat is negligible, its value was assumed to be equal to 1170 J/(kgK). Moreover, the latent heat was set to 395 611 J/kg, while the solidus and liquidus temperatures were equal to 923.42 K and 838.15 K, respectively. As described above, latent heat content ΔH including the latent heat varied according to Eq. (4). between the solidus and liquidus temperatures.

In the continuous casting process the liquid material flows into a mould (crystallizer). Inside the mould, the liquid material solidifies and is pulled out by withdrawal rolls along x-axis, see Figure 1. For this reason, the known boundary conditions were prescribed as in the real process [1]. Namely, at the top surface the velocity inlet was defined with the following values: inlet velocity was equal to the pull velocity $w_x = 0.001$ m/s, while the inlet temperature was equal to the liquid metal temperature. Moreover, as already mentioned on two side walls of the domain the symmetry planes were prescribed.

The second group of boundary conditions consisted of the estimated heat flux profiles defined on the other two side surfaces of the body. The ingot is usually additionally cooled by water sprayed over the surface outside the crystallizer. A production technology of the continuous casting strongly depends on the heat flux distribution along the cooled boundaries of an ingot. From the previous experience and literature [1], [5], [2], it was assumed that the heat flux varied linearly along the mould and exponentially along the water spray. For this reason, only three heat fluxes needed to be estimated.

In this work the heat flux distribution was defined by functions dependent on three estimated fluxes q_1, q_2 and q_3 and variable x (casting was carried along this direction). The heat flux distributions were specified in the following form:

$$x \in\ <0, d_m> \quad \Rightarrow$$
$$-f_1(x) = \frac{q_2 - q_1}{d_m} \cdot x + q_1$$

$$x \in\ <d_m, d_m + r> \quad \Rightarrow$$
$$-f_2(x) = \frac{q_3 - q_2}{r} \cdot x + q_2 + \frac{q_3 - q_2}{r} \cdot (d_m + r)$$

$$x \geq d_m + r \quad \Rightarrow$$
$$-f_3(x) = q_3 \cdot (0.85 \cdot \exp(60 \cdot (1.3 - x)) +$$
$$+ 0.621 - 0.465 \cdot x)$$

$$(6)$$

where d_m is the length of crystallizer, q_1 and q_2 are the values of the heat flux at the top and at the end of crystallizer, respectively. The variable q_3 indicates the heat flux at point just below the end of the mould.

At points where casting body sinks the mould, the heat flux "jump" appears. The linear function f_2 defining the heat flux distribution was assumed on a short segment (its the length was equal to $r = 0.015$m) under the end of the mould. Additionally, the exponential distribution was assumed on the part of the body that was cooling by sprayed water (function f_3).

In the problem presented the length of a crystallizer was 1 m which was approximately 20% of the solidified ingot length. The similar proportion of the ingot and the crystallizer lengths could be found in literature [1].

During the solidification, a process of contraction occurs in both mushy zone and solid part of the ingot. A change of volume increases rapidly with the temperature drop. This strongly affects the cooling conditions. Therefore, to simulate a realistic casting process the thermal contact resistance was considered as well. This can be summarized as follows: for each grid cell, a geometrical volumetric contraction was determined using polynomial temperature dependent functions. Then the volumetric contraction was used to calculate an air gap between two cooled side wall of the ingot and internal walls of the crystallizer. As a result, spatially local values of contraction distribution were obtained. The heat is transferred through the air gap by radiation and also natural convection. Therefore, a final distribution of the thermal contact resistance was computed as a sum of the inverse of the radiative and convective heat transfer coefficients. The radiative heat transfer coefficient was determined based on the radiative heat exchange between two vertical walls, while the convective heat transfer coefficient was computed using formulas for the Nusselt equations for the closed rectangular enclosures. Both these procedures are well known in the heat transfer literature. It is worth mentioning that the temperatures occurring in those algorithms were local temperatures of the boundary cell centres and boundary cell faces. The thermal contact resistivity distribution is presented in Fig. 2 and is defined as thermal contact resistance multiplied by the solid fraction and divided by the cell height of the wall-adjacent cell. All material properties were determined using algorithms described in [12].

The computations of the solidification process using the default parameters in Fluent turned out to be numerically
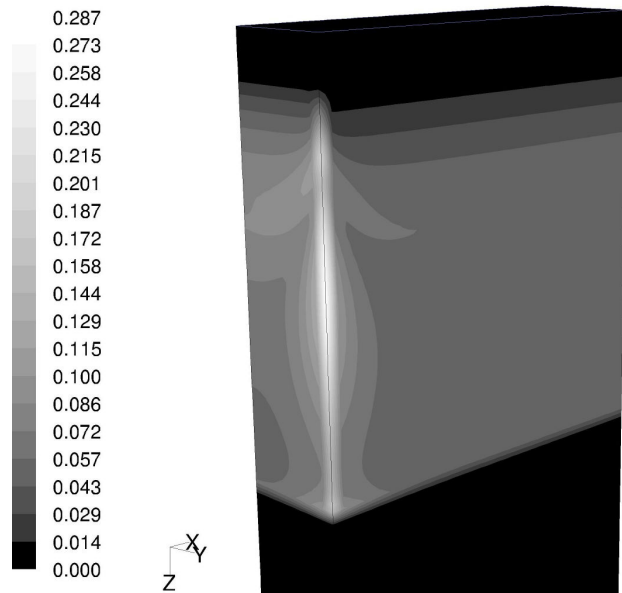

Fig. 2. The thermal contact resistivity in two cooled ingot walls.

unstable and led to disconvergence. For this reason, the direct problem was solved under unsteady conditions that significantly improved the stability of the iteration process. The time step size was increased gradually during calculations and its maximum value was equal to $\Delta t = 2$ s. The most effective inverse procedure was performed for the following parameters of the direct problem calculations in the iterative loop: the number of iterations in each time step equal to 10 and the number of time steps equal to 15.

III. INVERSE PROCEDURE

This model serves as a basis for the inverse problem discussed in detail in the remainder of the section.

Retrieving some unknown or lost information in the mathematical model of the direct heat transfer problem is the main object of the inverse analysis. This means that the incomplete mathematical description needs to be supplemented by measurements. In this work the boundary conditions were estimated by using numerically simulated temperatures measured inside the body. In practice, this kind of measurements can be obtained by immersing a set of thermocouples into the melt and letting them travel with the solidified material (until they are damaged). The use of the thermocouples is one of the most typical methods connected with temperature measurements in heat transfer problems [7]. Typically, the temperatures U_i are measured at some points inside the ingot and collected in the vector $\mathbf{U}$. On the other hand, it is very important to limit the number of sensors because of commonly known difficulties with data acquisition. Moreover, apart from valuable information each measurement session introduces some noise. The application of functions permits the modelling of the heat flux distribution using a much smaller number of design variables and in consequence the reduction in a number of sensors.

On the other hand the main difficulty of all inverse problems is its ill-posed nature. Because of this the number of measurements should be greater than the number of design variables (to make the problem overdetermined). Thus, in general, the inverse analysis leads to optimization procedures with the least squares calculations of the objective functions Δ. However, an additional term intended to improve stability usually needs to be used:

$$
\begin{aligned}
\Delta \;=\; & (\mathbf{T}^* - \mathbf{U})^T \, \mathbf{W}^{-1} \, (\mathbf{T}^* - \mathbf{U}) + \\
& + \left(\mathbf{Y} - \widetilde{\mathbf{Y}}\right)^T \mathbf{W}_Y^{-1} \left(\mathbf{Y} - \widetilde{\mathbf{Y}}\right) \rightarrow \min
\end{aligned} \tag{7}
$$

where vector $\mathbf{T}^*$ contains temperatures calculated at temperature sensor locations, $\mathbf{U}$ stands for the vector of temperature measurements and superscript T denotes the transpose matrices. The symbol $\mathbf{W}$ refers to the covariance matrix of measurements. This is a diagonal matrix with values of error in adequate location on diagonal. Thus, the contribution of more accurately measured data is stronger than those obtained with lower accuracy. The unknown variables are collected in vector $\mathbf{Y}$, known prior estimates in the vector $\widetilde{\mathbf{Y}}$, and $\mathbf{W}_Y$ stands for the covariance matrix of the prior estimates. It means that on a diagonal of matrix $\mathbf{W}_Y$ there are the estimated errors of the identified values. It was already found that the additional term in the objective function, containing prior estimates, plays a very important role in the inverse analysis, considerably improving the stability and accuracy of the inverse procedure [3].

Generally, the inverse problem is solved by building up a series of direct solutions which gradually approach the correct values of the design variables. This procedure can be expressed by the following main steps:

- make the boundary problem well-posed. This means that the mathematical description of the thermal process is completed by assuming arbitrary but known values $\mathbf{Y}^*$ (as required by the direct problem). In the study, different values of the starting distributions of the heat flux were tested. Results showed that they were independent on the initial profile of the heat flux on the boundary. For the results reported, the starting heat flux was uniform along the height of the domain and was equal to $250\,000$ W/m^2.

- solve the direct problem obtained above and calculate temperatures $\mathbf{T}^*$ at the sensor locations; compare these temperatures and measured values $\mathbf{U}$ and modify the assumed data $\mathbf{Y}^*$. The computations of the direct problem were performed in an unsteady state and tested with different values of a number of the time steps. The most effective procedure in terms of the total calculation time was obtained for the number of the time steps equal to 25 in each cycle. This means that the solution was only partly converged in a particular cycle. Obviously, the final values of the retrieved heat fluxes were obtained after a number of the cycles that guaranteed a fully converged solution of the direct problem.

In the paper the sensitivity analysis was applied to find the solution of the discussed inverse heat transfer problem. Generally the concept of sensitivity coefficients is utilized in this procedure [8]. The coefficients $\mathbf{Z}$ are derivatives of the measured quantity i.e. temperature T_i at certain location, with respect to the assumed and then identified input data Y_j:

$$
Z_{ij} = \frac{\partial T_i}{\partial Y_j} \tag{8}
$$

They provide a measure of each identified value and indicate how much it should be modified. Moreover, the sensitivity analysis helps one to determine which measurements are the most precious. Unfortunately, the measurement errors cause that "the best" sensor location is not unique.

Two different distributions of twenty sensors used for the temperature measurements were considered. In the first case, the measurement points were located in the vicinity to the top and bottom of the crystallizer, while in the second one sensors were uniformly distributed along the crystallizer. The obtained values of the temperatures and the sensitivity coefficients in both systems of sensor distributions produced very satisfactory results in the inverse procedure. In the paper the solution achieved for the uniformly distributed sensors was reported only, see Figure 1.

The sensitivity coefficients can be calculated by different techniques but the most effective one requires solution of adjoined boundary problem, obtained by a differentiation of the governing equation, the known boundary conditions and the boundary conditions consisting of the estimated heat fluxes with respect to the design variables.

In the computations of the sensitivity coefficients the domain included the solidified part of the ingot only. As a result, the direct sensitivity problem is formulated on the basis of the heat conduction equation in the following form:

$$
\nabla \cdot (k\nabla Z) = \boldsymbol{\nabla} \cdot \rho \boldsymbol{w} c_p Z + \frac{\partial}{\partial t}(\rho c_p Z) \tag{9}
$$

while the boundary conditions along the external boundary (for ith design variable) equals:

$$
-z_{1,i}(x) = \tfrac{\partial}{\partial q_i}\left(f_1(x)\right) \quad \text{if} \quad x \in\; < 0, d_m >
$$

$$
-z_{2,i}(x) = \tfrac{\partial}{\partial q_i}\left(f_2(x)\right) \quad \text{if} \quad x \in\; < d_m, d_m + r > \tag{10}
$$

$$
-z_{3,i}(x) = \tfrac{\partial}{\partial q_i}\left(f_3(x)\right) \quad \text{if} \quad x \geq d_m + r
$$

The boundary conditions on the top, bottom and the symmetry planes of the body were as in the original thermal problem, but homogeneous.

As already mentioned, in the considered case the three heat fluxes were estimated (compare equation (10)). In consequence, the sensitivity coefficients resulted in three systems of equations [5], [2]. Once calculated sensitivity coefficients were introduced into the objective function and as a result of its minimization the following system of equations was obtained:

$$
(\mathbf{Z}^T \mathbf{W}^{-1} \mathbf{Z} + \mathbf{W}_Y^{-1})\mathbf{Y} =
$$

$$
= \mathbf{Z}^T \mathbf{W}^{-1}(\mathbf{U} - \mathbf{T}^*) + (\mathbf{Z}^T \mathbf{W}^{-1} \mathbf{Z})\mathbf{Y}^* + \mathbf{W}_Y^{-1}\widetilde{\mathbf{Y}} \tag{11}
$$

where $\mathbf{Z}$ stands for the sensitivity coefficients matrix and $\mathbf{T}^*$ is the vector of temperatures at the sensor locations obtained by

solving the direct problem with trial heat fluxes $\mathbf{Y}^*$. The system (11) is obtained by minimization of the objective function (7) and introduction of Z by the Taylor series representation of temperature T (in the vicinity of temperature T^*). Using matrix notation and truncating the Taylor series after the first term one obtains

$$\mathbf{T} = \mathbf{T}^* + \mathbf{Z}\left(\mathbf{Y} - \mathbf{Y}^*\right) \qquad (12)$$

The solution of this set of equations resulted in a vector of the sought design variables (i.e. vector $\mathbf{Y}$). The objective was to estimate the components of the vector $\mathbf{Y}$ which uniquely described the heat flux distribution along boundary of ingot.

Above procedure was successfully applied for both boundary and geometry inverse problems in 2-D model [9]. For this reason, it was decided to use the above algorithm in 3-D case. For this kind of formulation, the inverse problem is solved by building up a series of direct solutions, which gradually approaches the correct values of the design variables. As mentioned in the previous section, in a particular cycle the solution was only partly converged (15 times steps, and 10 iterations per time step). This means that the final values of the retrieved heat fluxes were obtained after a number of the cycles.

IV. NUMERICAL RESULTS

In the study (because of assumptions reported in section II) a vector of the estimated variables contained three components i.e. $\mathbf{Y} = [q_1, q_2, q_3]$. In the numerical model (with air gap and mushy zone taken under consideration) the heat fluxes had the following values: $q_1 = -0.5$ MW/m^2, $q_2 = 0$ MW/m^2, $q_3 = -1.9$ MW/m^2 and for these values the temperatures at sensor points were calculated.

Because experimental tests are always burdened with errors, the numerically simulated measurements were obtained by adding to the temperature at sensor points random errors with uniform distribution.

One has to remember that the measurement errors considerably influence the results of the inverse thermal analysis and due to the ill-posed nature of the problem, the estimated heat fluxes might be very inaccurate. Therefore, the influence of the accuracy of measurements on the estimated heat fluxes was investigated.

Tests were performed for numerically generated measurements disturbed by 0.1% 0.5%, 1%, 2% and 5% error. Additionally, the calculations with "error" 0% were carried out to test the method. The results obtained have been presented in Table I.

It is easy to check that the average error of the estimated values (calculated as arithmetic mean of $\dfrac{|q_i^{est} - q_i^{model}|}{q_i^{model}}$, where q_i^{model} and q_i^{est} are the values of ith heat flux in numerical model and obtained at the end of iteration process, respectively) is approximately a half of the measurement error. Still better results can be found in the last column of Table I where the average errors of the temperatures calculated at sensor points are collected. One has to remember that in real problems a comparison of the measurements and

TABLE I
RESULTS OBTAINED FOR DIFFERENT LEVEL OF MEASUREMENTS ERROR.

	measurement error in %	estimated value in W/m^2	average error in sensors in K (in %)
q_1	0.0	-500 265	0.007
q_2		78	(0.0009)
q_3		-1 899 583	
q_1	0.1	-500 077	0.276
q_2		113	(0.0038)
q_3		-1 897 627	
q_1	0.2	-500 536	0.03
q_2		103	(0.0032)
q_3		-1 895 336	
q_1	1.0	-501 089	2.982
q_2		515	(0.3809)
q_3		-1 878 917	
q_1	2.0	-501 872	5.960
q_2		938	(0.7605)
q_3		-1 858 500	
q_1	5.0	-504 640	14.895
q_2		2 182	(1.8948)
q_3		-1 796 991	

temperatures calculated in the model is the only possibility. In the calculations presented here, the average difference at 20 points (for 1% error of measurements) is less than 1 K at the average temperature level of $800 - 900$ K. The values in the last column of Table I should be understood as the arithmetic mean of the error in all sensor points. The error in K is the absolute difference between temperature calculated at sensor point and measurement. The average percentage error is calculated as the averaging quotient of the absolute difference mentioned before and measurement.

Fig.3 presents a comparison of the temperatures at sensor locations calculated in the direct, fully liquid-solid model (taking an air gap into consideration), numerically simulated measurements (with errors not bigger than 2%), and the temperatures calculated for the retrieved boundary conditions in the inverse procedure.
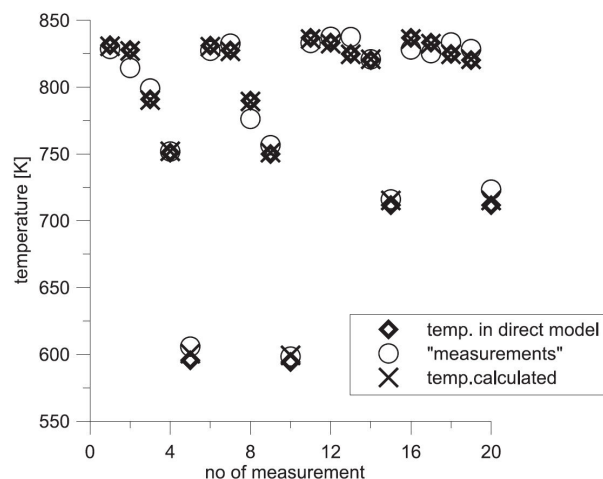
Fig. 3. The temperature values at sensor locations obtained in the iteration procedure.

As already mentioned, the computational procedure of re-

trieving the unknown values was carried out iteratively. Figure 4 presents the flow of this procedure for the measurement error 2% (character of the flow for other error levels is the same). It should be stressed that for different error levels the obtained results demonstrated similar accuracy and in all cases the stabilization of iteration process was observed after 80-100 iterations.
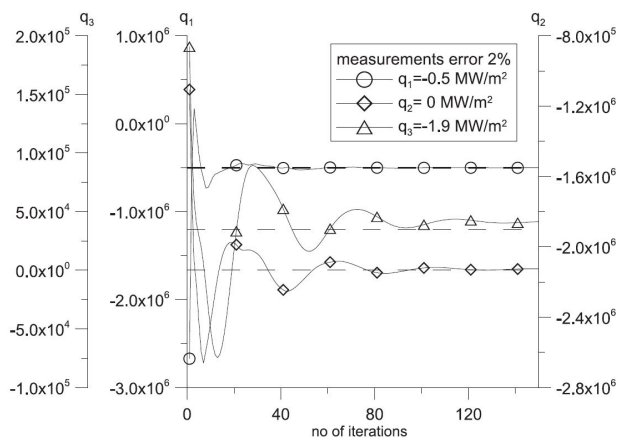

Fig. 4. The retrieved heat fluxes obtained in iteration procedure.

The big oscillations observed in first few steps can be reduced by properly selected absolute error of estimates (occurring in matrix $\mathbf{W}_Y$) and starting values. The final results do not depend on a choice of this values, only the computational time can be lengthened.

V. Conclusion

The problem was formulated as a 3-D inverse boundary problem in a continuous casting and was solved as a series of direct solutions, which gradually produced an accurate values of the designed variables. On the basis of subject literature, the heat flux distribution was approximated by linear and exponential functions inside and outside the crystallizer, appropriate. It considerably allowed the reduction of a number of the estimated values. The procedure developed for retrieving the cooling conditions turned out to be computationally very effective and independent on the starting value of the assumed boundary condition. A comparison of the measured and retrieved values showed a high accuracy of the computations. The satisfactory results were also obtained in calculations investigating the influence of the accuracy of measurements on the estimated heat fluxes. Some observations concerning the possibility of the calculation time reduction were also made. This paper discussed an identification procedure of the heat flux distribution along an ingot external boundary in continuous casting.

Acknowledgment

References

[1] J. M. Drezet, M. Rappaz, G. U. Grn and M. Gremaud *Determination of Thermophysical Properties and Boundary Conditions of Direct Chill-Calst Aluminium Alloys Using Inverse Methods* Metall. And Materials Trans. A **31** p.1627-1634, 2000.
[2] I. Nowak, A. J. Nowak and L. C. Wrobel, *Boundary and geometry inverse thermal problems in continuous casting*, Inverse Problems in Engineering Mechanics IV (eds. M. Tanaka and G.S. Dulikravich), Nagano, Japan: Elsevier p.21-32, 2003.
[3] A. J. Nowak, *BEM Approach to Inverse Thermal Problems*, Chapter 10 in Boundary Integral Formulations for Inverse Analysis (eds. Ingham D B, Wrobel L C), Southampton UK: Comp. Mech. Publications, 1997.
[4] *Fluent Product Documentation*, www.fluent.com
[5] K. Kurpisz and A. J.Nowak, *Inverse Thermal Problems*, Southamption, UK: Comp. Mech. Publications, 1995.
[6] V. R. Voller and C. Prakash, *A Fixed-Grid Numerical Modeling Methodology for Convection-Diffusion Mushy Region Phase-Change Problems*, Int. J. Heat Mass Transfer, **30** p.1709-1720, 1987.
[7] J. A. Dantzig, *Improvement transient response of termpocouple sensors*, Rev. Sci. Instrum. **56(5)** p.723-725, 1985.
[8] J. V. Beck, B. Blackwell, *Inverse Problem* Handbook of Numerical Heat Transfer (eds. Minkowycz W J, Sparrow E M, Schneider G E and Pletcher R H), New York: Wiley Intersc., 1988.
[9] I. Nowak, A. J. Nowak and L. C. Wrobel, *Tracking of Phase Change Front for Continuous Casting - Inverse BEM Solution*, Inverse Problems in Engineering Mechanics II, (eds. M. Tanaka and G.S. Dulikravich), Nagano, Japan: Elsevier, p.71-80, 2000.
[10] R. Conde, M. T. Parra, F. Castro, J. M. Villafruella, M. A. Rodriguez, C. Mendez, *Numerical model for two-phase solidification problem in a pipe*, Applied Thermal Engineering, **24**, p.2501-2509, 2004.
[11] T. A. Blase, Z. X. Guo, Z. Shia, K. Long, W. G. Hopkins, *3D conjugate heat transfer model for continuous wire casting*, Materials Science and Engineering, **365**, p.318-324, 2004.
[12] Z. Guoa, N. Saunders, A. P. Miodownik, J. -P. Schille, *Modelling of materials properties and behaviour critical to casting simulation*, Materials Science and Engineering, **413**, p.465-469, 2005.